Operational and Structural Optimization of Multi-Carrier Energy Systems*

Martin Geidl† and Göran Andersson
Power Systems Laboratory, ETH Zurich, 8092 Zurich, Switzerland

February 2006

Abstract

This paper presents an approach for the combined optimization of energy systems including multiple energy carriers such as electricity, natural gas, and district heat. Power flow and conversion between the different energy infrastructures are described as multi-input multi-output coupling, what enables simple analysis and optimization of the flows. While previous work deals with operational optimization (multi-carrier optimal dispatch and power flow), this paper focuses on optimization of the couplings between the different networks, i.e. the structure of the system.

Keywords

Multiple energy carriers, power system modeling, power system optimization, structural optimization, distributed generation

1 Introduction

Increasing utilization of gas-fired and other distributed generation, especially co- and trigeneration [1, 2], is expected to affect both the technical and economical operation of energy systems. The conversion between different energy carriers (e.g. natural gas into electricity and heat) establishes a coupling of the corresponding power flows resulting in system interactions. Therefore investigations concerning co- and trigeneration should cover all involved energy carriers, e.g. electricity, natural gas, and district heat.

The combined modeling and optimization of multiple energy carrier power flow has recently been addressed in a number of publications, e.g. [3, 4, 5, 6, 7, 8, 9, 10]. Different models have been developed and used for different purposes. While approximated models are used e.g. in [4] for optimizing the flows through an energy supply chain, [5] deals with detailed steady-state power flow equations for natural gas and electricity, since the model is intended to be used for optimal dispatch in a real system. The approach presented in [9, 10] aims at providing a tool for the development of a greenfield approach for future power systems. Thus a rather approximate model is developed for describing power flow and conversion of different energy carriers. The model is based on the concept of *energy hubs*. As indicated in figure 1, an energy hub connects loads with power delivery systems or primary sources of energy.

*Presented at International Conference on Future Power Systems, Amsterdam, The Netherlands, 2005; published in European Transactions on Electrical Power, vol. 16, no. 5, 2006.

†Correspondence to: Martin Geidl, Power Systems Laboratory, ETH Zurich, Physikstrasse 3, ETL G 24.1, 8092 Zurich, Switzerland; phone: +41 (0)44 632 65 77; fax: +41 (0)44 632 12 52; email: geidl@eeh.ee.ethz.ch

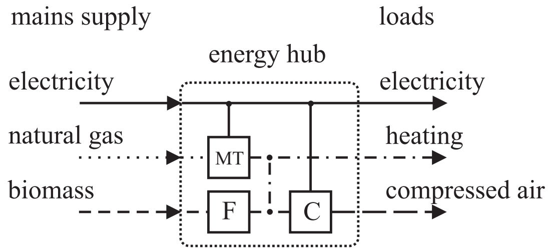

Figure 1: Example of an energy hub that interfaces loads with power delivery infrastructures. The hub contains a micro turbine (MT), a furnace (F), and a compressor (C).

Previous work is dedicated to power flow and operational optimization models [9, 10]. In this paper the structural optimization of power flow couplings is discussed. The paper is structured as follows. In section 2, the power flow model is reviewed and discussed from the perspective of structural optimization. The optimization problem is then derived in section 3 and demonstrated using examples in section 4. Section 5 gives a short summary and discussion.

2 System Modeling

The system model outlined in the following paragraphs is basically developed in [9, 10]. We extend the discussion pointing out certain mathematical properties which are important for topological optimization. Furthermore, the network flow model is enhanced by directly including line losses in the equations.

2.1 Basic Modeling Concept

We consider the mixed energy carrier power system as a combination of different networks (e.g. electricity, natural gas) and energy hubs (e.g. demand-side cogeneration). The difference between networks (links/lines) and hubs is that the hubs couple flows of different energy carriers, whereas network flows are assumed to be decoupled. When considering a systems of interconnected hubs, models for power conversion (within the hubs) as well as for power transmission (through the networks) are required. Accordingly, we state the model in two parts: a model for energy hubs is presented in section 2.3, a network model is discussed in section 2.5.

In order to obtain equations which are both sufficiently general and accurate enough for describing all types of energy flow, the following assumptions and simplifications are made:

- The system is in a steady state.
- Power flow is characterized through power, efficiency, and energy; no other quantities are used.
- The model incorporates conservations laws (conservation of flow) but no constitutional laws (e.g. relation between voltage and current).

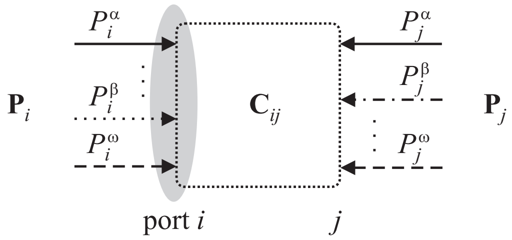

Figure 2: Single energy hub establishing a coupling between ports i and j.

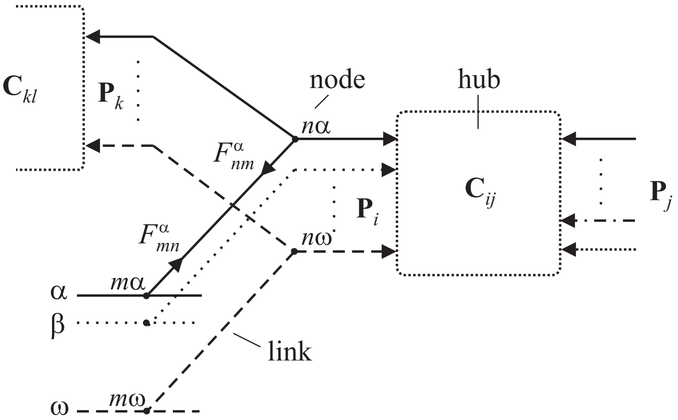

Figure 3: System of interconnected energy hubs including hubs, links, and nodes.

The simplified model, which corresponds to a network flow or transportation model [11], is believed to provide sufficient accuracy for overall system design studies. However, for other purposes detailed power flow models may be required to obtain meaningful results.

2.2 Nomenclature

Before discussing the mathematical model, we start with some definitions and conventions (see figures 2 and 3):

- Small Greek letters denote members of the set of energy carriers: $\alpha \in \mathcal{E} = \{\text{electricity}, \text{hydrogen}, \text{steam}, \ldots\}$.
- Small Latin letters denote members of the set of port numbers: $i \in \mathcal{P} = \{1, 2, \ldots\}$.
- The set of couplings contains pairs of the related port numbers: $(i, j) \in \mathcal{C} = \{(1, 2), (3, 4), \ldots\}$, where $i, j \in \mathcal{P}$.
- P denotes power exchanged at a hub port, F denotes power flow on a line, and L is used for line losses.
- Superscript letters are used to indicate energy carriers, subscript letters indicate port numbers.

2.3 Power Conversion

As indicated in figure 2, we consider 2-port hubs establishing port-to-port couplings $(i, j) \in \mathcal{C}$. The powers exchanged at ports i and j can be stated in vectors $\mathbf{P}_i$ and $\mathbf{P}_j$, respectively. The relation between the power vectors can be formulated as:

$$\underbrace{\begin{bmatrix} P_j^\alpha \\ \vdots \\ P_j^\omega \end{bmatrix}}_{\mathbf{P}_j} + \underbrace{\begin{bmatrix} c_{ij}^{\alpha\alpha} & \cdots & c_{ij}^{\omega\alpha} \\ \vdots & \ddots & \vdots \\ c_{ij}^{\alpha\omega} & \cdots & c_{ij}^{\omega\omega} \end{bmatrix}}_{\mathbf{C}_{ij}} \underbrace{\begin{bmatrix} P_i^\alpha \\ \vdots \\ P_i^\omega \end{bmatrix}}_{\mathbf{P}_i} = \mathbf{0} \tag{1}$$

$\mathbf{C}_{ij}$ is called the *coupling matrix*, it maps the powers from port i to port j. Note that this matrix is generally not invertible, i.e. (1) is underdetermined. This is an important feature which reflects the degrees of freedom which enable optimization. If $\mathbf{C}_{ij}$ is regular, then there is a unique solution for the input flows given required outputs. The entries of $\mathbf{C}_{ij}$ can be derived from the converter efficiencies and the topology of the coupling (see section 2.4). Two important characteristics of the coupling matrix are obvious:

- Since no power can be gained by converting one form of power α into another one β, all entries of the coupling matrix are limited according to minimal/maximal efficiency:
$$0 \leq c_{ij}^{\alpha\beta} \leq 1 \quad \forall\,(i,j) \in \mathcal{C}, \alpha, \beta \in \mathcal{E} \tag{2}$$
- The sum of all outputs $\alpha, \beta, \ldots, \omega$ converted from a single input α has to be lower than or equal to the input. Thus each column-sum of the coupling matrix is limited:
$$0 \leq \sum_{\beta \in \mathcal{E}} c_{ij}^{\alpha\beta} \leq 1 \quad \forall\,(i,j) \in \mathcal{C}, \alpha \in \mathcal{E} \tag{3}$$

These properties of the coupling matrix will serve as inequality constraints in the optimization problem formulation (section 3.2).

2.4 Derivation of the Coupling Matrix

In this section we will shortly discuss how the coupling matrix can be derived for a given converter arrangement. Actually, the paper aims at finding the optimal coupling rather than stating the matrix for a given layout. But, as we will see later, knowledge about the construction of the coupling matrix is important when trying to interpret optimization results.

As mentioned above, the coupling matrix can be derived from the converter efficiencies and the topology of the coupling. Converter efficiencies can be assumed as constants or as functions of the converted power. The power flow through a device that converts power from α to β can be stated as

$$P^\beta = \eta^{\alpha\beta}(P^\alpha) \cdot P^\alpha \tag{4}$$

where $\eta^{\alpha\beta}(P^\alpha)$ is the power-dependent efficiency of the converter; P^α and P^β are the input and output powers, respectively. This type of equation as well as nodal equations are used to define the coupling matrix for a given converter arrangement.

A specific complication related to nodal equations comes up when considering input junctions where the total input flow of a certain energy carrier splits up and flows into several converters. In this case, the dispatch of the total input to the individual converters has to be defined by introducing so-called *dispatch factors*. The dispatch factor ν_{ik}^α defines how much of the total input P_i^α flows into a certain connected branch

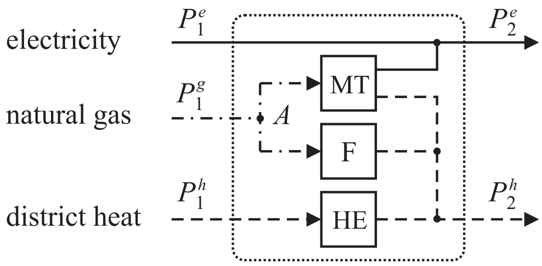

Figure 4: Example of a simple energy hub realized with a micro turbine (MT), a furnace (F), and a heat exchanger (HE).

k; $i \in \mathcal{P}$ and $\alpha \in \mathcal{E}$ identify the junction, and k is the consecutive branch number. Two basic properties of dispatch factors are:

- Since every branch carries only a part of the total input flow, all dispatch factors must be lower than or equal to one:

$$0 \leq \nu_{ik}^{\alpha} \leq 1 \quad \forall\, k, i \in \mathcal{P}, \alpha \in \mathcal{E} \tag{5}$$

- Due to conservation of power, the sum of all dispatch factors related to a junction must be equal to one:

$$\sum_{k} \nu_{ik}^{\alpha} = 1 \quad \forall\, i \in \mathcal{P}, \alpha \in \mathcal{E} \tag{6}$$

After discussing some modeling details in the preceding paragraphs, we will now focus on setting up the coupling matrix. As outlined in [10], the coupling matrix can be derived following a certain procedure:

a) Define power vectors at the involved ports.

b) Introduce dispatch factors at input junctions.

c) Express converter outputs as functions of the inputs.

d) State nodal power balance at output junctions.

e) Formulate the results in (1).

The following example should demonstrate the derivation of the coupling matrix including the introduction of dispatch factors.

■ Example: We will now state the coupling matrix for a simple but realistic coupling. Consider the combination of converters shown in figure 4. At port 1, electricity, natural gas, and district heat are provided. The power demanded from port 1 is converted and supplied to the load via port 2. The interface comprises a micro turbine (MT) which converts natural gas into electricity and heat, a furnace (F) which burns gas and provides heat, and a heat exchanger (HE) which interfaces the district heating network with the local heating system.

Following the items in the list above, we start by defining power vectors $\mathbf{P}_1 = \begin{bmatrix} P_1^e & P_1^g & P_1^h \end{bmatrix}^T$ and $\mathbf{P}_2 = \begin{bmatrix} P_2^e & P_2^h \end{bmatrix}^T$. Consider now the junction at the natural

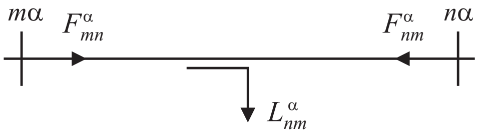

Figure 5: Power flow model for lossy lines.

gas input. Node A represents an input junction, therefore we introduce a dispatch factor ν which defines how much of the total gas input P_1^g is flowing into the MT:

$$P^g_{MT} = \nu P^g_1 \tag{7a}$$
$$P^g_F = (1-\nu)\, P^g_1 \tag{7b}$$

Expressing converter outputs as functions of their inputs and stating nodal power balance at junctions at the output side of the converters result in

$$P^e_2 = P^e_1 + \nu P^g_1 \eta^{ge}_{MT} \tag{8a}$$
$$P^h_2 = P^h_1 \eta^{hh}_{HE} + \nu P^g_1 \eta^{gh}_{MT} + (1-\nu) P^g_1 \eta^{gh}_F \tag{8b}$$

Finally, we can write (8) as a matrix equation:

$$\underbrace{\begin{bmatrix} P^e_2 \\ P^h_2 \end{bmatrix}}_{\mathbf{P}_2} = \underbrace{\begin{bmatrix} 1 & \nu\eta^{ge}_{MT} & 0 \\ 0 & \begin{smallmatrix}\nu\eta^{gh}_{MT} \\ +(1-\nu)\eta^{gh}_F\end{smallmatrix} & \eta^{hh}_{HE} \end{bmatrix}}_{\mathbf{C}_{12}} \underbrace{\begin{bmatrix} P^e_1 \\ P^g_1 \\ P^h_1 \end{bmatrix}}_{\mathbf{P}_1} \tag{9}$$

The dispatch factor ν represents a control variable for the coupling described by $\mathbf{C}_{12}(\nu)$. When modeling the efficiencies of the converter devices as functions of the converted power, the dispatch factor appears in the corresponding expressions, since the converter input depends on it. □

2.5 Power Transmission

Power flow on links (connecting the ports of different hubs) is modeled as outlined in figure 5. Conservation of power yields

$$F^{\alpha}_{mn} - L^{\alpha}_{mn} + F^{\alpha}_{nm} = 0 \tag{10}$$

The line losses can be expressed as a function of the terminal power: $L^{\alpha}_{mn} = f(F^{\alpha}_{mn})$. Losses in an electricity line, for example, can be approximated as a quadratic function of the power, whereas natural gas transmission losses grow with the cube of the flow [4]. Together with nodal equations, the line equations (10) can be summarized yielding a complete description of all α-flows:

$$\mathbf{A}^{\alpha}\mathbf{F}^{\alpha} - \mathbf{L}^{\alpha} - \mathbf{P}^{\alpha} = \mathbf{0} \tag{11}$$

where $\mathbf{A}^{\alpha}$ is the branch-nodal incidence matrix of the network containing elements $\{0, \pm 1\}$. The vector $\mathbf{F}^{\alpha}$ contains all line flows of the energy carrier α, $\mathbf{L}^{\alpha}$ contains flow-dependent line losses, and $\mathbf{P}^{\alpha}$ contains powers of the form α exchanged at the hub ports.

3 System Optimization

3.1 Optimization Problems

Different energy carriers are provided at the hub inputs, and certain loads are required at the hub outputs. The converters within the hub may establish redundant paths resulting in a certain degree of freedom in the supply of the hub. Consider for example the energy hub shown in figure 4. The electricity load can be met by consuming all power from the corresponding input or by converting a part or all of the load power from natural gas using the micro turbine, resulting in decreased electricity and increased natural gas input. Note that whenever the micro turbine is utilized for generating electricity, heat is produced simultaneously. Consider also that usually all involved energy carriers offered at the hub input are characterized by different costs, related emissions, etc. This situation raises questions concerning optimal power flow and conversion. Basically, two different types of optimization problems can be identified:

- *Operational optimization* aims at optimizing the power flows and conversions within the hubs and the networks for a given topology $(\mathbf{A}^{\alpha}, \mathbf{C}_{ij})$ according to a certain objective. Results include the network and hub power flows as well as the power dispatch on the converters within the hubs.
- With *topological* or *structural optimization* we mean the optimization of the hub-internal characteristics, i.e. finding the optimal coupling matrix according to load requirements and a certain objective. So far, we optimize only the topology of the hubs $(\mathbf{C}_{ij})$, not the networks ($\mathbf{A}^{\alpha}$ are given). Results include the network and hub power flows as well as the theoretically optimal coupling matrices.

The operational optimization of hub systems is elaborated in [9, 10]. In the following paragraphs, we develop an approach for topological optimization.

3.2 Topological Optimization

The topological optimization problem can be stated as a nonlinear constrained optimization problem defined by an objective function and constraints.

In standard optimal dispatch approaches, the total energy cost in the system should be minimized [12]. Other common criteria are plant emissions [13] and transmission security [14]. With regard to a technological realization of the couplings, certain criteria which include characteristics of the coupling matrix could be included in the objective function. Finally, line power flows should be included in order to minimize transmission losses. The different objectives can be merged in a composite objective function including the port powers $\mathbf{P}_i$, the coupling matrices $\mathbf{C}_{ij}$, and the line flows $\mathbf{F}^{\alpha}$. Equality constraints arise from the hub and system power flow equations (1) and (11), respectively. Inequalities arise from power limitations of ports and links. We define their minimal and maximal values in vectors $\underline{\mathbf{P}}_i$, $\underline{\mathbf{F}}^{\alpha}$, $\overline{\mathbf{P}}_i$, and $\overline{\mathbf{F}}^{\alpha}$, respectively. Additional inequalities are given by the characteristics of the coupling matrix (2) and (3). Finally, the problem can be mathematically stated as (12).[1]

[1]Maximization problems can be transformed into minimization problems using $\max_x f(x) = -\min_x -f(x)$ [15].

$$
\begin{array}{ll}
\text{Minimize } f\left(\mathbf{P}_i, \mathbf{C}_{ij}, \mathbf{F}^\alpha\right) & \\
\text{subject to} & \\
\mathbf{P}_j + \mathbf{C}_{ij}\mathbf{P}_i = \mathbf{0} & \forall\, (i,j) \in \mathcal{C} \\
\mathbf{A}^\alpha\mathbf{F}^\alpha - \mathbf{L}^\alpha - \mathbf{P}^\alpha = \mathbf{0} & \forall\, \alpha \in \mathcal{E} \\
\underline{\mathbf{P}}_i \leq \mathbf{P}_i \leq \overline{\mathbf{P}}_i & \forall\, i \in \mathcal{P} \\
\underline{\mathbf{F}}^\alpha \leq \mathbf{F}^\alpha \leq \overline{\mathbf{F}}^\alpha & \forall\, \alpha \in \mathcal{E} \\
0 \leq c_{ij}^{\alpha\beta} \leq 1 & \forall\, (i,j) \in \mathcal{C}, \alpha, \beta \in \mathcal{E} \\
0 \leq \sum\limits_{\beta \in \mathcal{E}} c_{ij}^{\alpha\beta} \leq 1 & \forall\, (i,j) \in \mathcal{C}, \alpha \in \mathcal{E}
\end{array}
\tag{12}
$$

Given are the output powers $\mathbf{P}_j$, the topologies of the networks $\mathbf{A}^\alpha$, and the limits $\underline{\mathbf{P}}_i, \overline{\mathbf{P}}_i, \underline{\mathbf{F}}^\alpha$ and $\overline{\mathbf{F}}^\alpha$. The solution of the optimization problem contains the optimal coupling matrices $\mathbf{C}_{ij}$, the hub inputs $\mathbf{P}_i$ and network flows $\mathbf{F}^\alpha$.

The problem (12) represents a nonlinear, inequality-constrained optimization problem. If (12) is of convex nature, nonlinear programming [15, 16] techniques can be employed for the solution. Depending on the actual structure and the numerical condition of the equations in (12), two complications may appear:

- The problem may have an infinite number of (equally optimal) solutions, whereas not all of them are technically reasonable.
- The solution may depend on the starting point (initial values) of the optimization routine.

A simple ad hoc solution to overcome the problem of infinite solutions is to include a criterion related to the coupling matrix in the objective function. The second problem can be eliminated by starting the optimization routine at technically reasonable values, what includes the risk that unexpected, unconventional solutions may remain undiscovered.

■ Example: We optimize the connection of a three-dimensional load $\mathbf{P}_2 = -\begin{bmatrix} 1 & 1 & 1 \end{bmatrix}^T$ pu (electrical/chemical/thermal) to the three input networks, searching for the optimal coupling matrix $\mathbf{C}_{12}$ and power inputs $\mathbf{P}_1$ (see figure 2). The objective function to be minimized is stated as the sum of the squared input powers. The optimal input yielding a minimal objective is evident: $\mathbf{P}_1 = \begin{bmatrix} 1 & 1 & 1 \end{bmatrix}^T$ pu. It can be achieved with different coupling matrices $\mathbf{C}_{12}$, for example:

$$
\begin{bmatrix} 1 & 0 & 0 \\ 0 & 1 & 0 \\ 0 & 0 & 1 \end{bmatrix}; \begin{bmatrix} 0 & 0 & 1 \\ 0 & 1 & 0 \\ 1 & 0 & 0 \end{bmatrix}; \frac{1}{3}\begin{bmatrix} 1 & 1 & 1 \\ 1 & 1 & 1 \\ 1 & 1 & 1 \end{bmatrix}; \frac{1}{2}\begin{bmatrix} 0 & 1 & 1 \\ 1 & 0 & 1 \\ 1 & 1 & 0 \end{bmatrix} \tag{13}
$$

All matrices result in the same optimum, and there is an infinite number of other optimal solutions for $\mathbf{C}_{12}$. However, in this case the coupling described by the very left matrix is possibly the most reasonable one to implement, since it corresponds to directly connecting inputs and outputs. Realization of the second matrix for instance would require a thermal-electrical conversion which is usually less efficient and more expensive than a transmission line. The fourth matrix establishes the coupling without any direct connections, all input powers are converted into other forms. □

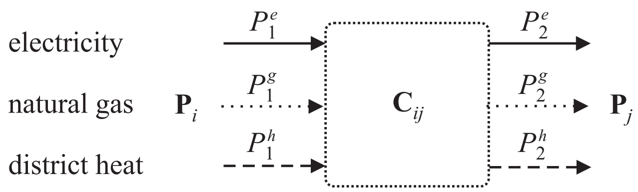

Figure 6: Example hub connected to electricity, natural gas, and district heating systems.

Table 1: Penalty function coefficients.

energy carrier α	a_1^α in pu^{-1}	a_2^α in pu^{-2}	a_3^α in pu^{-3}
electricity	2	0.05	0
natural gas	1	0	0.10
distr. heat	1	0	0.20

4 Examples

The presented optimization approach should now be demonstrated in two examples. Both of them were implemented using commercially available optimization software [17].

4.1 Single Energy Hub

Figure 6 shows a 2-port hub connected to electricity, natural gas, and district heating networks at the input side (port 1). The same energy carriers are demanded by the loads at the output (port 2). The relation between in- and output is $\mathbf{P}_2 = \mathbf{C}_{12}\mathbf{P}_1$.

We will now determine the optimal coupling matrix $\mathbf{C}_{12}$ and power input $\mathbf{P}_1$ for a given output $\mathbf{P}_2$. The penalty to be minimized is defined as a polynomial function of the input powers:

$$f(\mathbf{P}_1) = \sum_{\alpha \in \mathcal{E}} \sum_{n=1}^{3} a_n^\alpha \left(P_1^\alpha\right)^n \tag{14}$$

Table 1 gives the parameters a_n^α assumed for this example. The values are chosen based on common energy prices and loss behavior of the related carrier.

Table 2 shows the resulting optimal input for different required loads. Figure 7 shows the corresponding optimal coupling matrices. In order to enhance interpretability and clearness of the results, the matrix entries are displayed according to a color

Table 2: Example cases and results.

case	required $\mathbf{P}_2^T$ in pu	optimal $\mathbf{P}_1^T$ in pu
a)	[1 1 1]	[0.00 1.76 1.24]
b)	[1 0 1]	[0.00 1.17 0.83]
c)	[2 0 2]	[0.77 1.89 1.34]
d)	[1 0 2]	[0.00 1.76 1.24]
e)	[1 0 5]	[2.51 2.04 1.45]
f)	[2 0 10]	[7.84 2.44 1.72]

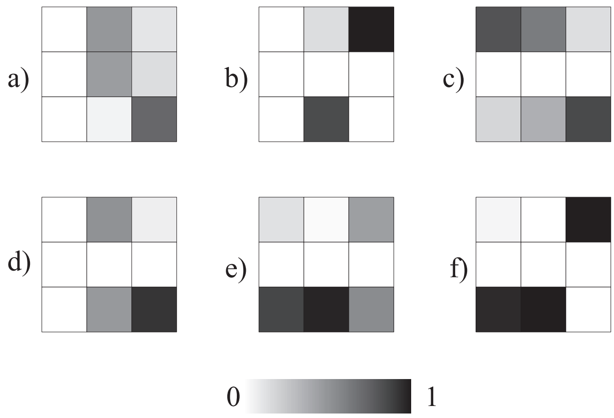

Figure 7: Color-mapped results for optimal $\mathbf{C}_{12}$.

map. From the theoretical results of the optimization, a technological representation (i.e. hub layout) can be derived that establishes the desired optimal coupling. Consider for example case d). Natural gas and heat are demanded from the networks to meet the load. The optimal coupling matrix shows non-zero elements for conversions from gas to electricity ($c_{12}^{ge} = 0.52$), gas to heat ($c_{12}^{gh} = 0.48$), heat to electricity ($c_{12}^{he} = 0.07$), and heat to heat ($c_{12}^{hh} = 0.93$). A converter layout that has the potential to realize this coupling could be based on a combined heat and power plant (CHP), which converts natural gas into electricity and heat with efficiencies c_{12}^{ge} and c_{12}^{gh}, i.e. 52% and 48%, respectively. c_{12}^{hh} could be realized by directly connecting the heat load (and the thermal CHP output) to the district heating network. Since the first column of $\mathbf{C}_{12}$ does not contain non-zero elements, there is no need to connect to the electricity network.

For case b), d), and f) interpretation of the results in terms of technological implementation can be carried out in a straightforward way based on empirical data. However, considering case a), c), or e) shows that advanced methods have to be used to identify topologies/technologies that comply with the desired optimum.

4.2 System of Interconnected Hubs

Consider the 3-bus electricity and natural gas networks in figure 8 which have to supply electricity, natural gas, and heat loads located at nodes 2 and 3. The loads are connected to the output port of the corresponding hub (2′ and 3′, respectively):

$$\mathbf{P}_{2'}^{T} = \left[\begin{array}{ccc} 1 & 1 & 2 \end{array} \right] \text{ pu}; \ \mathbf{P}_{3'}^{T} = \left[\begin{array}{ccc} 1 & 0 & 3 \end{array} \right] \text{ pu} \tag{15}$$

The electricity network is supplied by the generators $G1$ (slack) and $G2$, whose output is limited between 0.2 and 0.8 pu. The gas network is fed by a single source S. Besides the network infeeds, there are two smaller local sources of biomass at node 2 (B, max. 0.5 pu) and heat at node 3 (H, max. 1 pu). Line losses are modeled as quadratic/cubic functions of the flow, the corresponding loss coefficients are given in table 3.

The objective to be minimized is basically stated as the cost of energy input (considering all sources). In order to achieve technically reasonable results and to avoid the problems mentioned in section 3.2, we reduce the penalty by the sum of the diagonal

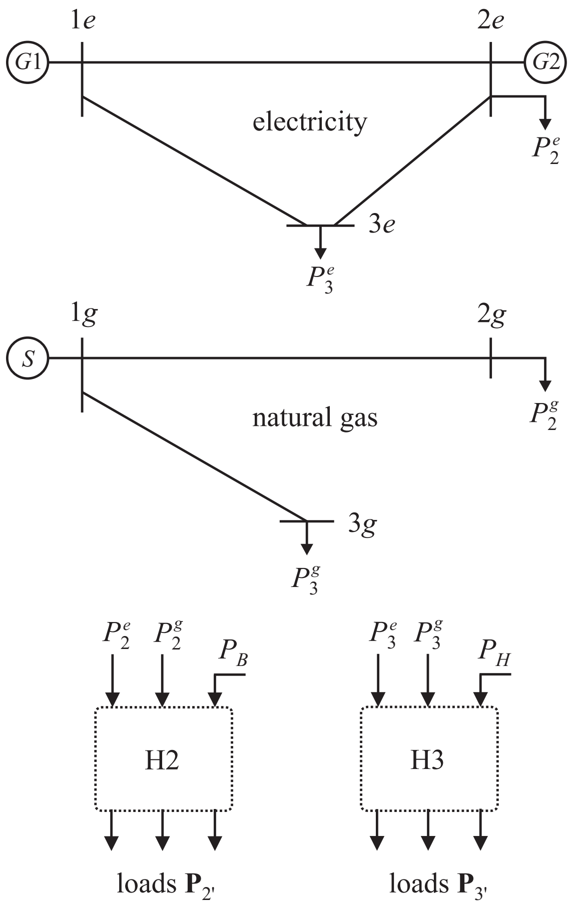

Figure 8: Example system with energy hubs at nodes 2 and 3.

Table 3: Network data.

link	length	loss coefficient
$1e$–$2e$	6 pu	0.006 pu^{-2}
$1e$–$3e$	4 pu	0.004 pu^{-2}
$2e$–$3e$	3 pu	0.003 pu^{-2}
$1g$–$2g$	6 pu	0.014 pu^{-3}
$1g$–$3g$	4 pu	0.010 pu^{-3}

Table 4: Penalty function coefficients.

source i	a_1^i in pu^{-1}	a_2^i in pu^{-2}	a_3^i in pu^{-3}
$G1$	8	0.003	0
$G2$	9	0.005	0
S	5	0	0.5
B	4	0	0
H	4	0	0

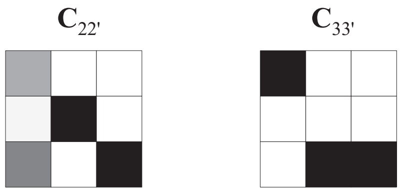

Figure 9: Color-mapped results for the optimal coupling matrices.

elements (trace) of the coupling matrices:

$$f(P^s, \mathbf{C}_{22'}, \mathbf{C}_{33'}) = \sum_{s \in \mathcal{S}} \sum_{n=1}^{3} a_n^s \left(P^s\right)^n - \mathrm{tr}\left(\mathbf{C}_{22'}\right) - \mathrm{tr}\left(\mathbf{C}_{33'}\right) \tag{16}$$

where $\mathcal{S} = \{G1, G2, S, B, H\}$ is the set of sources; P^s is the power delivered by source $s \in \mathcal{S}$. The values of a_n^s used in this example are given in table 4. Note that the formulation (16) intrinsically includes network losses, since the sources have to compensate for them. The optimal coupling matrices of hubs 2 and 3 ($\mathbf{C}_{22'}$ and $\mathbf{C}_{33'}$, respectively) describing the couplings established by these hubs can now be determined using the proposed optimization model.

The resulting optimal matrices are

$$\mathbf{C}_{22'} = \begin{bmatrix} 0.383 & 0 & 0 \\ 0.042 & 1 & 0 \\ 0.575 & 0 & 1 \end{bmatrix}; \ \mathbf{C}_{33'} = \begin{bmatrix} 1 & 0 & 0 \\ 0 & 0 & 0 \\ 0 & 1 & 1 \end{bmatrix} \tag{17}$$

Figure 9 gives a graphical illustration of $\mathbf{C}_{22'}$ and $\mathbf{C}_{33'}$. From the results a technological realization (converter layout) for the hubs can be derived that approximately establishes the theoretically optimal coupling. To realize the coupling described by $\mathbf{C}_{22'}$, direct connections linking all inputs and outputs are necessary in hub 2, what means that biomass has to be converted into heat. Additionally, a conversion from electricity to heat has to be implemented, what is technically possible with very high efficiencies close to 100%. About 58% of the electric input should be used for producing heat (what corresponds to a dispatch factor of 0.58). The comparably low entry representing conversions from electricity to gas can be neglected. Hub 3 should be equipped with direct connections for electricity and heat, and a device that converts gas into heat. Ideally, this device should operate with 100% efficiency; practical installations will of course show significantly lower efficiencies.

In figure 10 the resulting hub input flows are shown. Note that both local sources (biomass and heat) are utilized at their limits. Power from these sources is not transported via networks, therefore no losses occur from their use. The remaining power

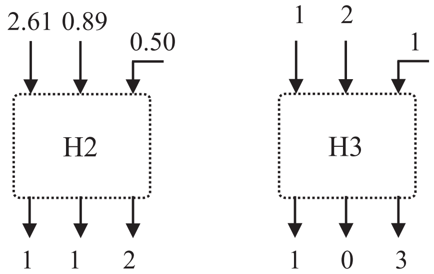

Figure 10: Given loads and resulting hub inputs (all values in pu).

comes from the network infeeds: $P^{G1} = 3.44$ pu, $P^{G2} = 0.2$ pu (lower limit), and $P^{S} = 3$ pu.

The results are optimal for the given specific load situation. For system design investigations, different load scenarios should be investigated. It is also possible to perform the optimization for a certain load profile, e.g. load power over a day.

5 Discussion and Conclusion

An approach for topological optimization of multiple energy carrier systems was developed which is based on the conceptual idea of energy hubs. It enables to determine the theoretically optimal interface between certain energy infrastructures and loads. For demonstration purposes, the approach was examined using simple example scenarios.

Calculating the theoretical optimum is considered as a first step in the development of a system design method, which identifies the technology requirements. A procedure that finds a technological representation which (approximately) corresponds to the mathematical result is subject to future work.

Finally, the following conclusions can be drawn:

- Modeling power conversion as an input-output coupling enables simple optimization of power flow and conversion in multi-carrier systems.
- The model for operational optimization can be extended and used for structural optimization, i.e. for determining the ideal connections/couplings between different energy infrastructures.
- Interpretation of the results is not a straightforward task. Mixed-integer programming techniques could be employed to determine optimal hub structures based on a given set of hub elements.

6 List of Symbols

i, j	port number
m, n	node number
k	branch number
s	source, member of $\mathcal{S}$
α	energy carrier, member of $\mathcal{E}$
$\mathcal{E}$	set of energy carriers
$\mathcal{P}$	set of port numbers
$\mathcal{C}$	set of port-to-port couplings
$\mathcal{S}$	set of energy sources
P_i^α	power of the form α exchanged at port i
P^s	power delivered by source s
F_{mn}^α	line power flow of α from node m to n
L_{mn}^α	line losses of α between node m and n
$\eta^{\alpha\beta}$	energy efficiency of conversion from α to β
$c_{ij}^{\alpha\beta}$	coupling factor describing α to β conversion from port i to j
ν_{ik}^α	dispatch factor related to carrier α, port i, and branch k
$\mathbf{P}_i$	power vector of port i
$\mathbf{C}_{ij}$	coupling matrix from port i to port j
$\mathbf{A}^\alpha$	connectivity matrix of the network carrying α
$\mathbf{F}^\alpha$	vector of line flows of the form α
$\mathbf{L}^\alpha$	vector of losses of the form α
$\mathbf{P}^\alpha$	vector of port powers of the form α
$\underline{\mathbf{P}}_i, \overline{\mathbf{P}}_i$	vector of minimal/maximal power exchange at port i
$\underline{\mathbf{F}}^\alpha, \overline{\mathbf{F}}^\alpha$	vector of minimal/maximal line flows in the system α
a_n^α	penalty function coefficient of n-th order for carrier α
a_n^s	penalty function coefficient of n-th order for source s

References

[1] D. Hinrichs, "Cogeneration," in *Encyclopedia of Energy*. Elsevier Inc., 2004, p. 581.

[2] J. Hernandez-Santoyo and A. Sanchez-Cifuentes, "Trigeneration: an alternative for energy savings," *Applied Energy*, vol. 76, no. 1-3, pp. 219–227, 2003.

[3] B. Bakken *et al.*, "Simulation and optimization of systems with multiple energy carriers," in *Proc. of the 1999 Conference of the Scandinavian Simulation Society (SIMS)*, Linköping, Sweden, 1999.

[4] I. Bouwmans and K. Hemmes, "Optimising energy systems—hydrogen and distributed generation," in *Proc. of the Second International Symposium on Distributed Generation: Power System and Market Aspects*, Stockholm, Sweden, 2002.

[5] S. An, Q. Li, and T. W. Gedra, "Natural gas and electricity optimal power flow," in *Proc. of IEEE PES Transmission and Distribution Conference*, Dallas, USA, 2003.

[6] E. M. Gil *et al.*, "Modeling integrated energy transportation networks for analysis of economic efficiency and network interdependencies," in *Proc. of North American Power Symposium (NAPS)*, Rolla, USA, 2003.

[7] J. Söderman and F. Pettersson, "Structural and operational optimisation of distributed energy systems," *Applied Thermal Engineering*, in press, corrected proof, 2005.

[8] O. D. de Mello and T. Ohishi, "An integrated dispatch model of gas supply and thermoelectric systems," in *Proc. of 15th Power Systems Computation Conference (PSCC)*, Liège, Belgium, 2005.

[9] M. Geidl and G. Andersson, "Optimal power dispatch and conversion in systems with multiple energy carriers," in *Proc. of 15th Power Systems Computation Conference (PSCC)*, Liège, Belgium, 2005.

[10] ——, "A modeling and optimization approach for multiple energy carrier power flow," in *Proc. of IEEE PES PowerTech*, St. Petersburg, Russian Federation, 2005.

[11] F. Glover, D. Klingman, and N. V. Phillips, *Network Models in Optimization and Their Applications in Practice.* Wiley, 1992, ISBN 0-471-57138-5.

[12] A. J. Wood and B. F. Wollenberg, *Power Generation, Operation, and Control*, 2nd ed. Wiley, 1996, ISBN 0-471-58699-4.

[13] J. W. Lamont and E. V. Obessis, "Emission dispatch models and algorithms for the 1990s," *IEEE Transactions on Power Systems*, vol. 10, no. 2, pp. 941–947, 1995.

[14] B. Stott, O. Alsac, and A. J. Monticelli, "Security analysis and optimization," *Proc. of the IEEE*, vol. 75, no. 12, pp. 1623–1644, 1987.

[15] R. Fletcher, *Practical methods of optimization*, 2nd ed. Wiley, 1987, ISBN 0-471-91547-5.

[16] H. W. Kuhn and A. W. Tucker, "Nonlinear programming," in *Proc. of the Second Berkeley Symposium on Mathematical Statistics and Probability.* Berkeley, USA: University of California Press, 1951.

[17] The Mathworks Inc., "Optimization toolbox," website, available at http://www.mathworks.com/products/optimization/, last accessed at 12th October 2005.

Acknowledgement

The work presented in this paper has been performed within the framework of the research project Vision of Future Energy Networks. The authors would like to thank ABB, Areva, VA Tech/Siemens, and the Swiss Federal Office of Energy for supporting this project.

Authors' Biographies

Martin Geidl was born in Wels, Austria. After he received a Dipl.-Ing. degree in electrical engineering from the Graz University of Technology, Austria, in 2003, je joined the Power Systems Laboratory of the Swiss Federal Institute of Technology (ETH), Zurich, Switzerland, where he is working towards a PhD. His research is dedicated to modeling and optimization of multiple energy carrier systems. He is a student member of the IEEE.

Göran Andersson was born in Malmö, Sweden. He obtained his MSc and PhD degree from the University of Lund in 1975 and 1980, respectively. In 1980 he joined ASEA, now ABB, HVDC division in Ludvika, Sweden, and in 1986 he was appointed full professor in electric power systems at the Royal Institute of Technology (KTH), Stockholm, Sweden. Since 2000 he is full professor in electric power systems at the Swiss Federal Institute of Technology (ETH), Zurich, Switzerland, where he heads the Power Systems Laboratory. His research interests are in power system analysis and control, in particular power system dynamics and issues involving HVDC and other power electronics based equipment. He is a member of the Royal Swedish Academy of Engineering Sciences and Royal Swedish Academy of Sciences and a Fellow of IEEE.